








Article

Anthropogenic Activity in the Topo-Climatic Interaction of the Tapajós River Basin, in the Brazilian Amazon

Vânia dos Santos Franco ^{1,2,*}, Aline Maria Meiguins de Lima ¹, Rodrigo Rafael Souza de Oliveira ³, Everaldo Barreiros de Souza ¹, Giordani Rafael Conceição Sodré ⁴, Diogo Correa Santos ², Marcos Adami ⁵, Edivaldo Afonso de Oliveira Serrão ² and Thaianie Soeiro da Silva Dias ¹

¹ Programa de Pós-Graduação em Ciências Ambientais, Universidade Federal do Pará, Belém 66075-110, Brazil; ameiguins@ufpa.br (A.M.M.d.L.); everaldo@ufpa.br (E.B.d.S.); thaianie.dias@ig.ufpa.br (T.S.d.S.D.)

² Instituto Tecnológico Vale, Desenvolvimento Sustentável, Belém 66055-090, Brazil; diogo.correa@pq.itv.org (D.C.S.); edivaldo.serrao@pq.itv.org (E.A.d.O.S.)

³ Departamento de Geografia, Universidade do Estado do Pará, Belém 66050-540, Brazil; rodrigo.oliveira@uepa.br

⁴ Faculdade de Meteorologia, Universidade Federal do Pará, Belém 66075-110, Brazil; giordani@ufpa.br

⁵ Instituto Nacional de Pesquisas Espaciais—INPE, São José dos Campos 12227-010, Brazil; marcos.adami@inpe.br

* Correspondence: vania.franco@pq.itv.org or vsanfranco@yahoo.com.br

Abstract: This research aimed to analyze the relationship between deforestation (DFT) and climatic variables during the rainy (CHU+) and less-rainy (CHU−) seasons in the Tapajós River basin. Data were sourced from multiple institutions, including the Climatic Research Unit (CRU), Center for Weather Forecasts and Climate Studies (CPTEC), PRODES Program (Monitoring of Brazilian Amazon Deforestation Project), National Water Agency (ANA) and National Centers for Environmental Prediction/National Oceanic and Atmospheric Administration (NCEP/NOAA). The study assessed anomalies (ANOM) in maximum temperature (TMAX), minimum temperature (TMIN) and precipitation (PREC) over three years without the occurrence of the El Niño–Southern Oscillation (ENSO) atmospheric–oceanic phenomenon. It also examined areas with higher DFT density using the Kernel methodology and analyzed the correlation between DFT and climatic variables. Additionally, it assessed trends using the Mann–Kendall technique for both climatic and environmental data. The results revealed significant ANOM in TEMP and PREC. In PREC, the highest values of ANOM were negative in CHU+. Regarding temperature, the most significant values were positive ANOM in the south, southwest and northwestern regions of the basin. Concerning DFT density, data showed that the highest concentration was of medium density, primarily along the highways. The most significant correlations were found between DFT and TEMP during the CHU− season in the Middle and Lower Tapajós sub-basins, regions where the forest still exhibits more preserved characteristics. Furthermore, the study identified a positive trend in TEMP and a negative trend in PREC.

Keywords: rainfall; air temperature; deforestation



Citation: Franco, V.d.S.; Lima, A.M.M.d.; Oliveira, R.R.S.d.; Souza, E.B.d.; Sodré, G.R.C.; Santos, D.C.; Adami, M.; Serrão, E.A.d.O.; Dias, T.S.d.S. Anthropogenic Activity in the Topo-Climatic Interaction of the Tapajós River Basin, in the Brazilian Amazon. *Hydrology* **2024**, *11*, 82. <https://doi.org/10.3390/hydrology11060082>

Academic Editors: Kleoniki Demertzi, Vassilis Aschonitis, Mavromatis Theodoros and Ioannis Pytharoulis

Received: 20 March 2024

Revised: 26 April 2024

Accepted: 27 April 2024

Published: 13 June 2024



Copyright: © 2024 by the authors. Licensee MDPI, Basel, Switzerland. This article is an open access article distributed under the terms and conditions of the Creative Commons Attribution (CC BY) license (<https://creativecommons.org/licenses/by/4.0/>).

1. Introduction

Deforestation (DFT) raises significant concerns worldwide among researchers and society due to its adverse impacts on the environment, climate and health [1,2]. The commitment to climate-related studies resulting from deforestation is driven by the ongoing occurrences of extreme events on the planet, such as floods, severe droughts, heatwaves and cold spells [3,4].

Research has concluded that the increase in extreme heat in North America and Europe is associated with the effects of DFT [5]. As a consequence of degradation in the Amazon, future simulation studies conducted in South America show an increase in air temperature

(TEMP), a decrease in precipitation (PREC) in the region and a significant reduction in forested areas [6,7].

The Amazon is globally renowned for its forests, abundant freshwater resources and mineral wealth. However, over the past few decades, the region has undergone significant transformations that have led to the degradation of a substantial portion of its forest [8,9].

The combination of land-use activities and the diverse forms of land alteration cover across the entire Amazon River basin territory (encompassing 6,403,450.74 square kilometers, including Brazil and the Andean countries) has raised various questions regarding its impact on regional water balance, its interaction with global systems and the resilience capacity of ecosystems in the face of changing conditions [10]. For example, research conducted by [11,12] indicates that deforestation can lead to an increase in flood runoff and a reduction in base flow in the region.

These transformations have sparked growing environmental concerns, particularly regarding the Amazon rainforest, due to the environmental services it provides, its biodiversity, water cycling and carbon storage [13,14]. The Amazon rainforest plays a vital role in maintaining the regional Amazonian climate, as well as other regions of the country, through the atmospheric transport of moisture [15].

An example of these transformations can be seen in the Tapajós River basin, which has experienced degradation in recent decades due to the pressure primarily caused by the expansion of agribusiness, including the increase in exports of agricultural and agro-industrial products [16]. Simultaneously with deforestation for agribusiness, highways are being constructed to create new routes to transport grains to the Port of Itaituba [17]. Additionally, the basin faces other issues such as the construction of hydroelectric dams, mining activities and logging.

The degradation is more pronounced in the Upper Tapajós (center-south of the basin) due to a higher concentration of activities (livestock farming, agriculture) and thus more pronounced deforestation in this portion of the basin. On the other hand in the Lower Tapajós (north of the basin), degradation has been increasing, as is the case in the northwest of the basin, where a significant portion of conservation units have seen a reduction in their boundaries due to degradation from mining and hydroelectric dam construction in the region [18]. The basin faces socio-environmental conflicts due to land disputes in many municipalities, such as Santarém, Itaituba, Novo Progresso and Sinop—located in the states of Pará and Mato Grosso, which drive deforestation in the region. [19].

The discussions regarding the consequences of massive forest conversion into pastures, leading to a decrease in rainfall in the Amazon and neighboring regions is another example [20], as well as in the southern part of the continent [21]. This transformation also contributes to increased temperature, severe droughts and floods [22]. Another measure is the substantial quantity of particles and gases emitted by wildfires, which profoundly affect regional and global climates [23,24].

As a result, this study aims to analyze the relationship between DFT and the variability of air temperature and precipitation and the climate in the CHU+ and CHU− seasons of the Tapajós River basin region, representing 7.7% of the Amazon River basin territory. Additionally, it seeks to assess the increases in DFT indices, their correlation with CHU+ and CHU− and determine if there is a statistical pattern between deforested areas, temperature (TEMP) and the amount of rainfall in the region.

The Tapajós basin exhibits significant contrasts in its natural resources, particularly regarding water and climate, which are subject to impacts due to disordered land use and land cover. Thus, possible changes in the studies of meteorological variables are suggested due to the degradation of the region, indicating a trend of increasing temperature and decreasing precipitation, especially in the portion of the basin that still has more preserved forest.

2. Materials and Methods

Located in the central Brazilian Amazon, the Tapajós River basin (Figure 1) covers an estimated area of 492,115.88 km². It spans the states of Mato Grosso (MT) (58%) and Pará (PA) (38%), with smaller portions in Amazonas (AM) (3%) and Rondônia (RO) (1%). This region holds significant socio-environmental importance. Not only is the Tapajós River the most significant tributary along the direct margin of the Amazon River, but it also serves as a contested space for territory and natural resources among indigenous communities, livestock farmers, timber extractors and settlers. The northern part of the basin is characterized by the Protected Areas. The Environmental Protection Area (APA) of Tapajós is located near the municipality of Itaituba and the Indigenous Lands. These lands occupy almost 25% of the territory in the state of Pará [18].

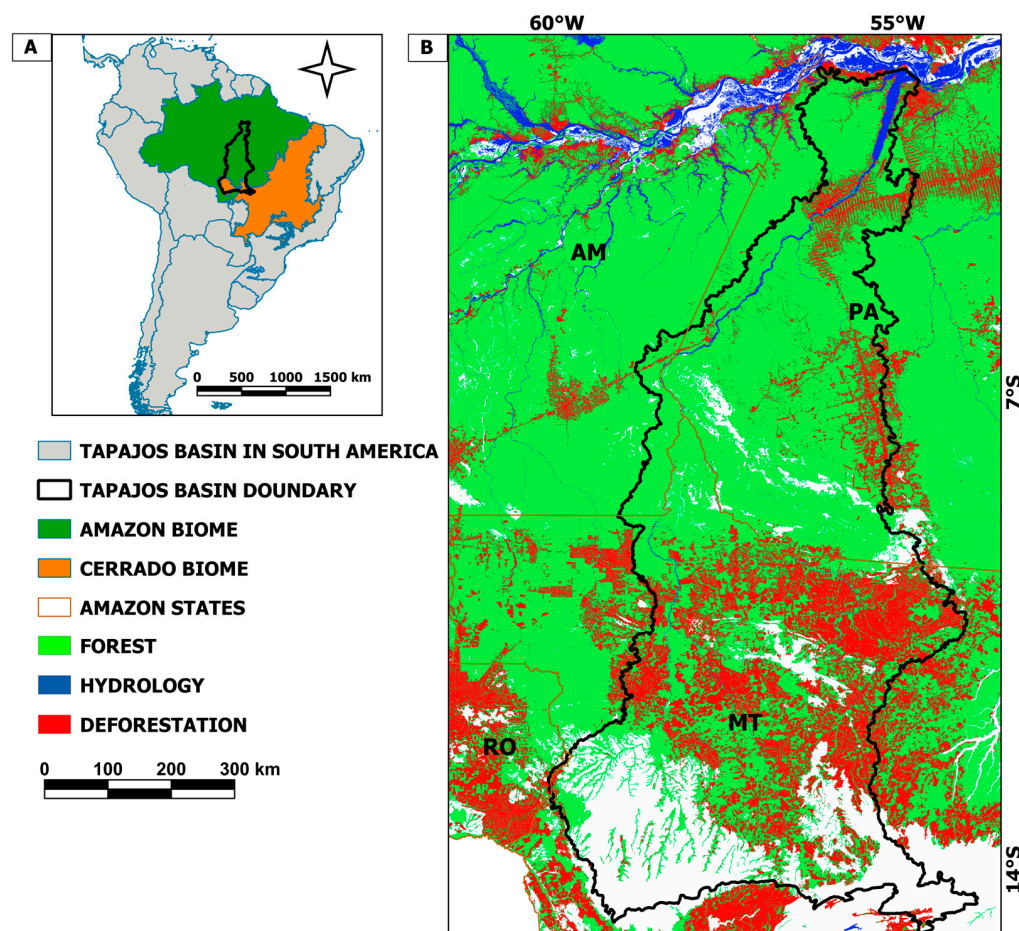


Figure 1. (A) Location of the Tapajós River basin in South America and (B) states of the Brazilian Amazon that make up the basin.

The Tapajós River basin plays a significant role as a contributor to the Amazon River basin, providing an average flow of 1400 m³/s, ranking the Tapajós River among the world's top 20 rivers in terms of discharge [25]. This context conflicts with the trend established in recent decades, marked by an economy focused on agribusiness [26–29], associated with the transportation of grains from the central region of the country, traveling along BR-163 to the Port of Santarém-PA [30].

This basin (Tapajós) holds several specificities, namely environmental and soil diversity, complex topography and vegetation consisting of two biomes (Figure 1A): the Amazon rainforest, which covers regions from the State of Pará to the north of Mato Grosso and the cerrado (savanna region in South America), located in the southern part of the basin. This landscape is associated with high average annual precipitation values (exceeding 1470 mm, sometimes reaching close to 2500 mm), with a gradual increase from the head-

waters towards the mouth, characterizing two seasons: a dry season (CHU−) from May to September and a rainy season from October to April, with May and October serving as transitional periods [31].

Regarding landscape characterization, the region exhibits high reliefs in the cerrado of the state of Mato Grosso and floodplain lands in the region of the state of Pará, demonstrating a significant altimetric difference with quite rugged terrain in the southern and central-eastern portions of the basin and an alluvial plain in the northern part (Figure 2A) [32].

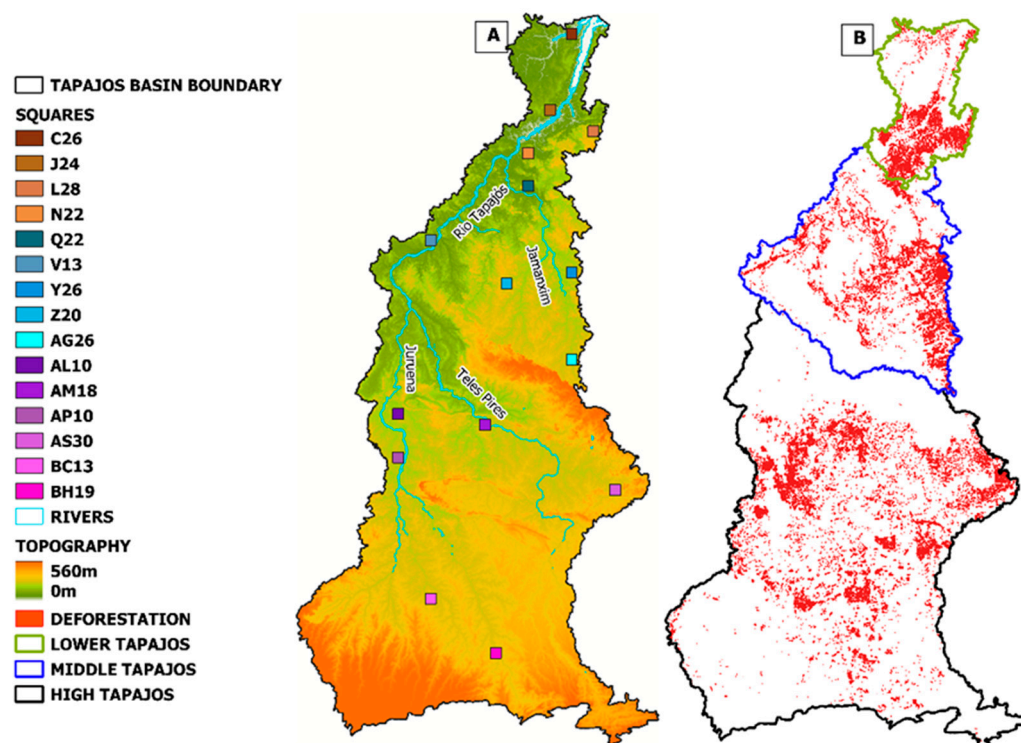


Figure 2. (A) Position of the squares in the regions of the Tapajós River basin and (B) deforested area in the three sub-basins: Lower, Middle and Upper Tapajós.

Cumulative PREC (precipitation) and average TMAX (maximum air temperature) and TMIN (minimum air temperature) data were used, seasonally (from November to April and May to October) obtained from the Climate Research Unit (CRU), derived from satellite estimates and in situ stations, were utilized. The data had a spatial resolution of approximately 21 km² (in TIF format) and were obtained from the WorldClim platform, a global weather and climate database, covering the period from 2000 to 2018. This dataset enabled the evaluation based on ANOM (anomalies) and the seasonality of CHU+ (rainy period) and CHU− (less rainy period).

Additionally, annual data on DFT from PRODES Program (Monitoring of Brazilian Amazon Deforestation Project) were utilized, available at (<http://terrabrasilis.dpi.inpe.br/> (accessed on 05 September 2022)). The chosen years 2010, 2013 and 2015 for PRODES's sample are representative of the deforestation.

Initially, the ANOM [33] was calculated according to Equation (1) for the CHU+ (2011–12, 2014–15 and 2016–17, November to April) and CHU− (2012, 2015 and 2017, May to September) seasons. The selection of these years is linked to the absence of influence from the ENSO phenomenon (El Niño–Southern Oscillation—El Niño and La Niña) in the data available in (<http://enos.cptec.inpe.br/> (accessed on 30 November 2022)):

$$X_i - \bar{X} \quad (1)$$

where X_i represents the collected value and \bar{X} the average value.

To calculate the ANOM, the arithmetic mean was first calculated (quotient of dividing the sum of the variable values by their numbers) via Equation (2). This result was added to the ANOM calculation (Equation (1)):

$$\bar{x} = \frac{\sum x_i}{n} \quad (2)$$

and standard deviation (which indicates how much each element of a series deviates from the series' mean), via Equation (3):

$$\sigma = \sqrt{\frac{\sum (x_i - \bar{x})^2}{n}} \quad (3)$$

where (σ) is the standard deviation, (x_i) elements of the set, (\bar{x}) the mean of the set and (n) the number of elements in the set.

Afterward, centroid maps were generated to illustrate areas with higher DFT density, for the years 2010, 2013 and 2015, using the Kernel density estimator [34]. Based on the concentration of DFT, the reclassified data defined three density levels: low (green), medium (yellow) and high (red).

The following steps were taken to investigate the degree of association/dependence between DFT and meteorological variables: Quantum GIS open-source software was used to extract the pixel grid from precipitation and air temperature data, with each grid cell within the basin measuring approximately 21 km² (Figure 2):

- (1) From this grid, time series of data were extracted pointwise at each grid cell, thus allowing for the creation of tables and the performance of statistical calculations. The sampling aimed for the greatest uniformity of the internal landscape of each grid cell, allowing the relationship to have a more direct correspondence with the dominant land cover (deforested area).
- (2) After selection, the total DFT value, accumulated PREC and average TMAX and TMIN for the CHU+ and CHU− stations were calculated for each grid cell from 2008 to 2018 (11 years). Microsoft Excel was used along with Pearson's correlation r tests (the quotient between covariance and the product of their standard deviations), Equation (4) and the coefficient of determination— R^2 (a measure (in percentage) of the amount of variation in one variable explained by the other; this is the square of Pearson's correlation coefficient) were applied to the tabulated data, which were then applied to the values of these variables [30,35]:

$$r_{X,Y} = \frac{COV(X,Y)}{\sigma_X \sigma_Y} \quad (4)$$

where COV represents covariance; X, Y represent the variables in question; and σ_X, σ_Y the standard deviation of the variable.

Additionally, the non-parametric Mann–Kendall test (applicable in cases where the values of the data X_i from a time series can be assumed as follows in Equation (5)) was applied to the tabulated data [36] for analyzing trends in PREC, TMAX and TMIN, CHU+ and CHU− stations (from 2000 to 2018) and DFT (from 2008 to 2020):

$$X_i = f(t_i) + \varepsilon_i \quad (5)$$

where $f(t)$ is a continuous temporal function, either monotonically increasing or decreasing, and the residue ε_i has the same distribution with zero mean, assuming that the variance of the distribution is constant over time.

3. Results

3.1. Climatological Normal and Precipitation and Temperature Anomaly

Figure 3 shows the average annual and seasonal (CHU+ and CHU−) PREC values for the period from 2000 to 2018. In the annual period, between 1700 and 2500 mm of precipitation are observed in the basin, with the highest values in the central regions of the basin and the lowest in the southwest. The CHU+ season shows higher PREC values in the east and central regions of the basin, with amounts exceeding 2000 mm. The lowest values are located in the north and southwest (between 1500 and 1700 mm). It can be seen that the basin's CHU− has the lowest PREC values in the center-south, with values below 300 mm. On the other hand the maximum PREC is found in the north, with a value of over 500 mm.

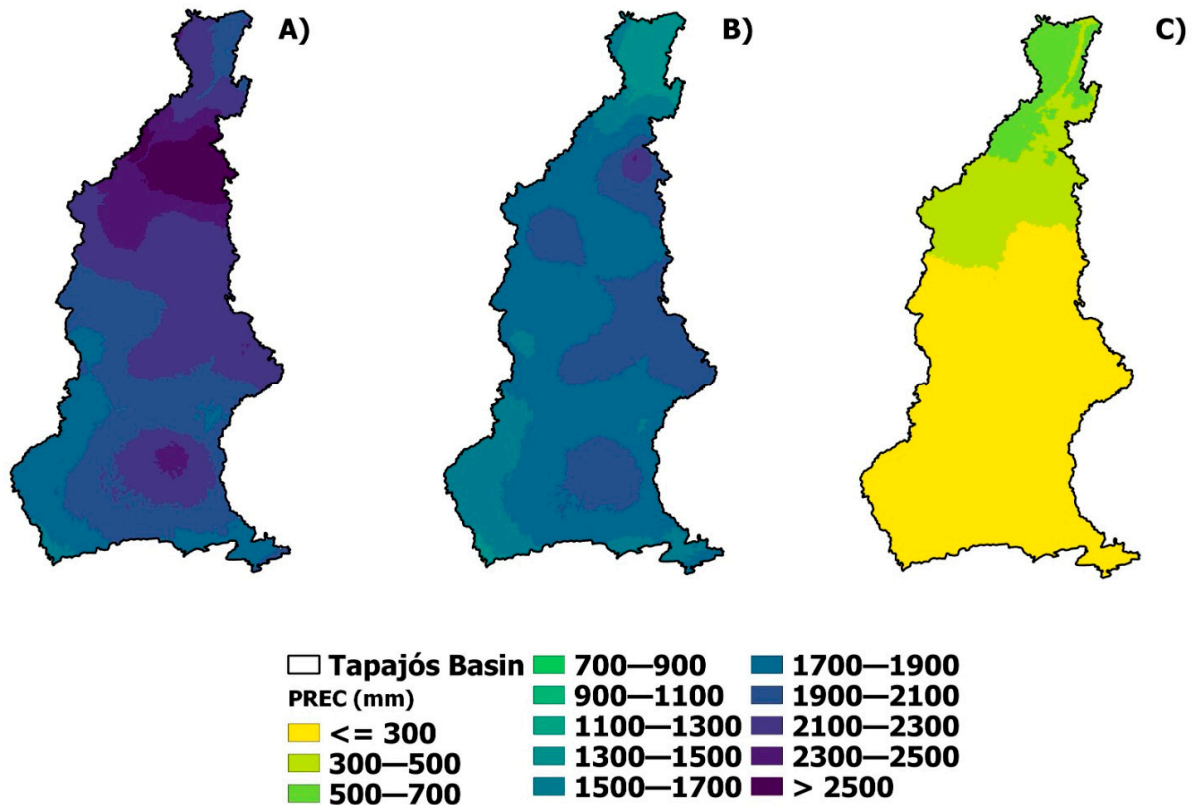


Figure 3. Average annual and seasonal values (CHU+ and CHU−) of PREC (2000 to 2018): (A) PREC annual, (B) CHU+ season and (C) CHU− season, respectively.

Figure 4 shows average annual and seasonal (CHU+ and CHU−) TMAX values for the period 2000 to 2018. The average annual temperature values are between 29 and 34 °C and above, with higher values in the central-eastern and western regions and lower values in the south. At CHU+, the average values are higher (between 31 and 32 °C) in the central-eastern and northwestern regions of the basin and lower (29 °C) in the northeastern and southwestern regions. The CHU− station shows values between 31 and over 34 °C, with the highest values in the central region of the basin and the lowest values in the extreme southern regions.

Figure 5 shows average annual and seasonal (CHU+ and CHU−) TEMP values for the period from 2000 to 2018. Average annual TEMP values are between 16 and 34 °C, with higher values in the north-central regions and lower values in the south of the basin. In CHU+, they are between 18 and over 24 °C, with the lowest values in the south and the highest in the north-central regions of the basin, especially in the northwest. In CHU−, the values are between 16 and 23 °C, with the lowest values in the far south and the highest in the central, northern and northwestern regions of the basin.

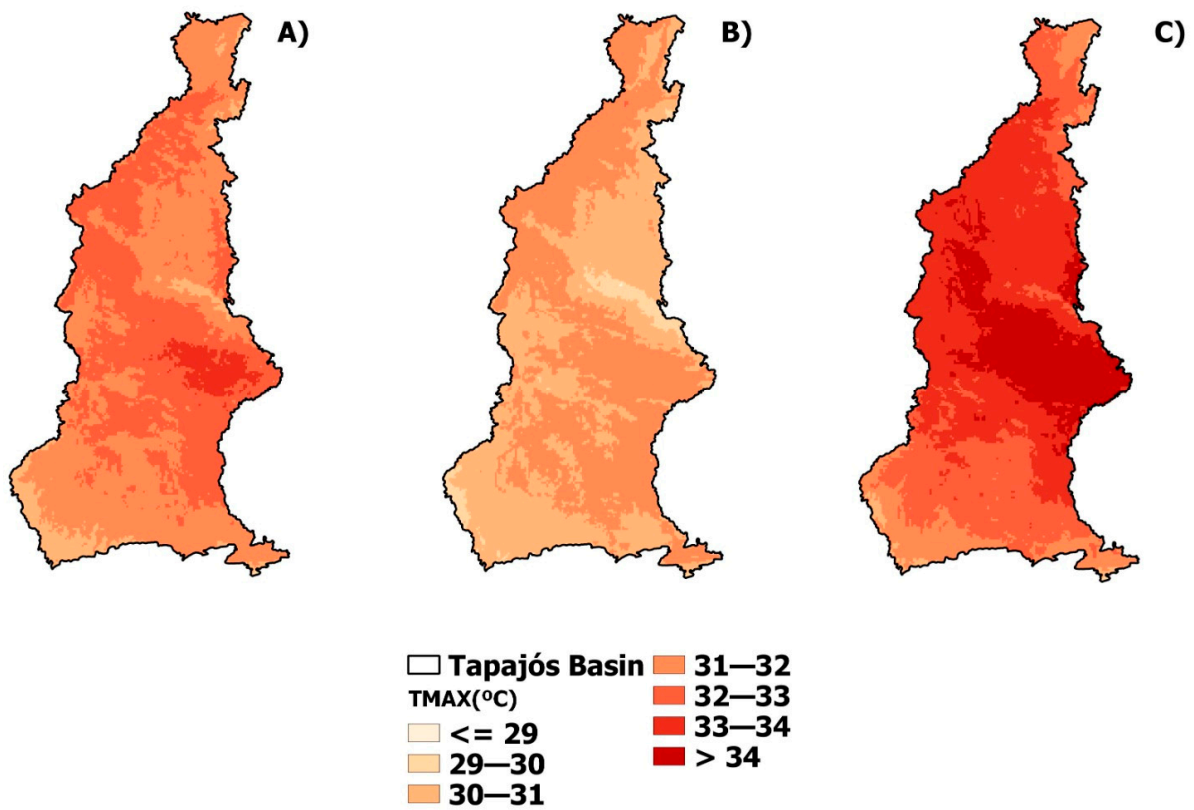


Figure 4. Average annual and seasonal (CHU+ and CHU–) TMAX values (2000 to 2018): (A) TEMP annual, (B) CHU+ season and (C) CHU– season, respectively.

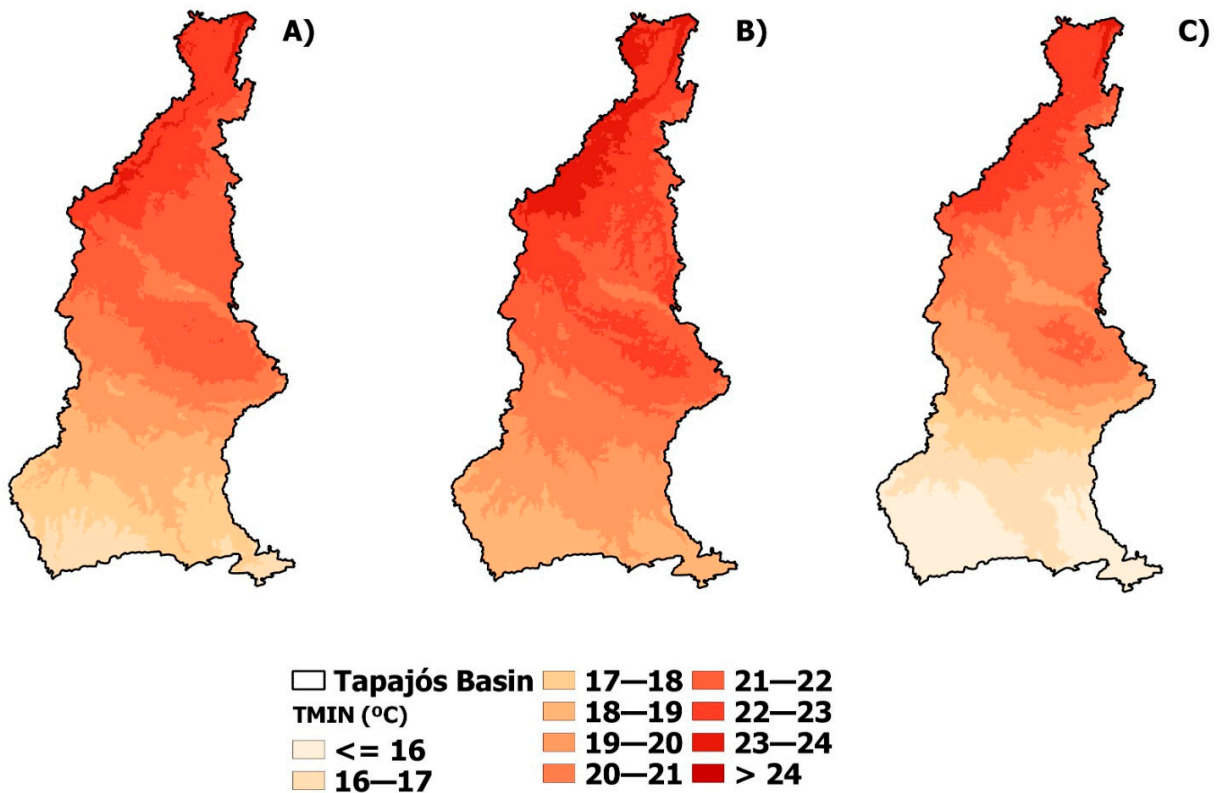


Figure 5. Average annual and seasonal (CHU+ and CHU–) TMIN values (2000 to 2018): (A) TEMP annual, (B) CHU+ season and (C) CHU– season, respectively.

The highest positive TMAX anomalies during the CHU+ season (Figure 6a–c) occurred from 2014 to 15 (Figure 6b) with values up to 1.0 °C in the southwest of the basin, a region located within the deforestation arc. Conversely, in 2011–12, negative anomalies of up to 0.4 °C were observed in the southeast and northeastern regions (Figure 6a), while positive anomalies of up to 0.6 °C were recorded in the southeast (Figure 6c).

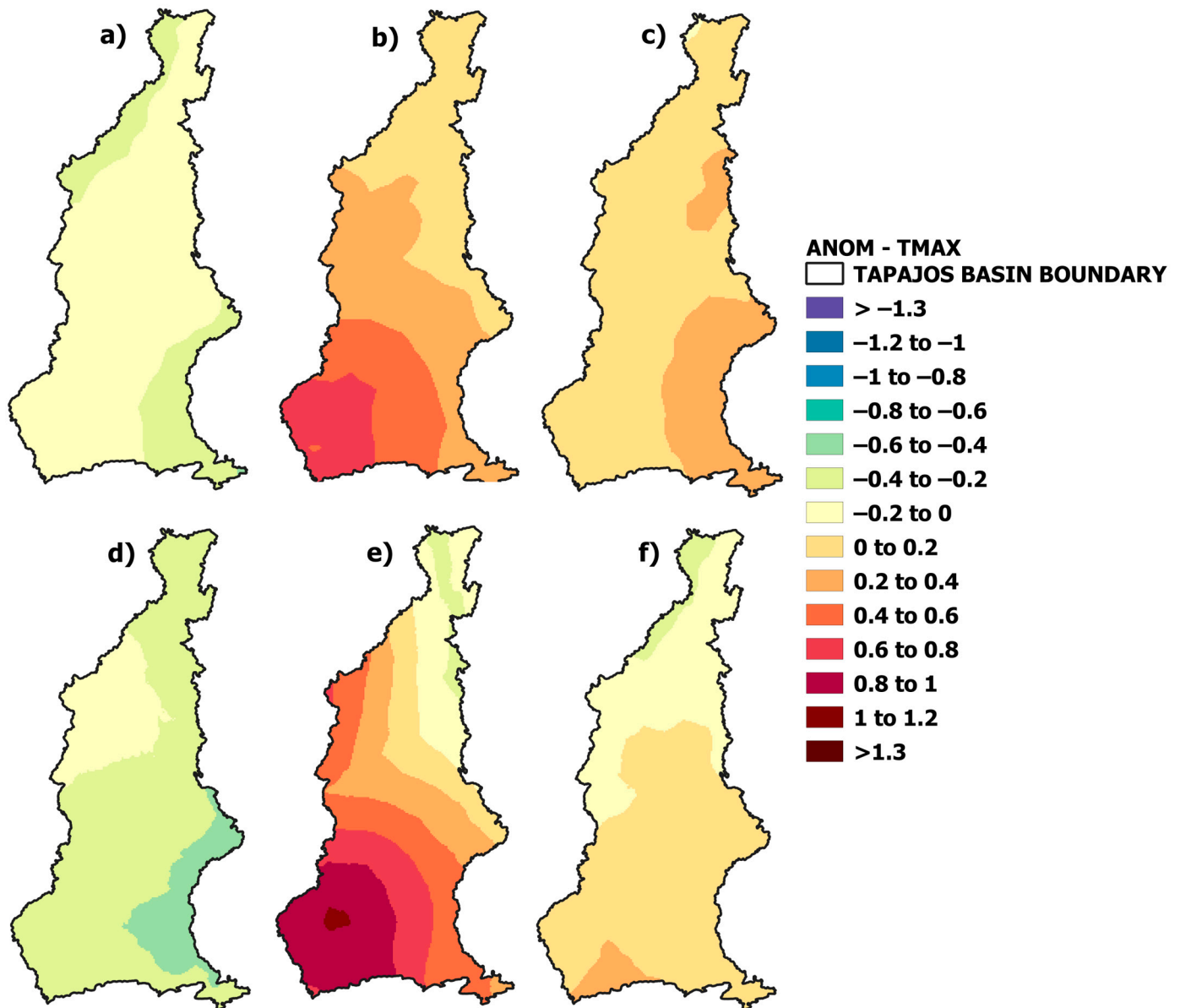


Figure 6. Maximum temperature seasonal anomaly for CHU+ (November to April) and CHU– (May to September) stations: (a–c) correspond to the CHU+ season of 2011–12, 2014–15 and 2016–17 and (d–f) correspond to the CHU– season of 2012, 2015 and 2017, respectively.

In the CHU– season (Figure 6d–f), negative ANOM values occurred across almost the entire basin in 2012, reaching up to 0.6 °C (Figure 6d) in the southeast. In 2015 (Figure 6e), positive ANOM values were noticeable across most of the basin, exceeding 1.3 °C in the southwestern region, except in the far north, where negative values were observed. The same ANOM value were observed in the northern region in 2017 (Figure 6f), with positive values of up to 0.4 °C in other areas, particularly in the southernmost part of the basin.

Table 1 shows the descriptive statistics (mean and standard deviation) of PREC and temperature for CHU+ and CHU–. Furthermore, the highest average TMAX occurred

during the 2014–2015 period in both seasons, while the lowest PREC was observed in the same period. Conversely, the lowest temperature was recorded during 2011–2012 (Table 1). The most significant variation in TMAX was observed between the CHU– periods, reaching 0.7 °C when comparing the average of the CHU– season in 2012 with that of 2015. In the CHU+ season, this increase was 0.5 °C. Regarding the standard deviation of TMAX, it remained at 0.4 in all three periods of the CHU+ season and averaged 1.0 in the CHU– season.

Table 1. Descriptive statistical analysis of the season variability of the CHU+ (2011–2012, 2014–2015 and 2016–2017) and CHU– (2012, 2015, 2017) states of the Tapajós River basin.

	PREC		TMAX		TMIN	
	CHU+	CHU–	CHU+	CHU–	CHU+	CHU–
Year	2011–2012 (CHU+)/2012 (CHU–)					
Average	1835.6	242.9	30.8	33.2	20.9	19.0
Standard deviation	131.3	111.7	0.4	1.0	1.4	2.4
Year	2014–2015 (CHU+)/2015 (CHU–)					
Average	1816.8	237.8	31.3	33.9	21.3	19.7
Standard deviation	206.7	116.8	0.4	0.9	1.3	2.0
Year	2016–2017 (CHU+)/2017 (CHU–)					
Average	1897.6	246.2	31.1	33.5	21.2	21.2
Standard deviation	126.2	111.3	0.4	1.0	1.4	1.4

Like TMAX (Figure 6), TMIN also exhibits a positive ANOM value predominance (Figure 7). Positive anomalies are observed in the CHU+ season (Figure 7b,c) in the southeast, southwest and northwestern regions (in all three periods) with values up to 0.8 °C. However, during the CHU+ season in 2011–2012, anomalies ranging between –2 °C and 0 °C were observed in a large part of the basin, reaching as low as –0.4 °C in the southeast.

In the CHU– season, the region with negative anomalies (Figure 7d) was reduced compared to the CHU+ season in the southeast. In other areas, especially in the northwestern region, positive anomalies were prevalent. During the CHU– seasons of 2015 and 2017, there was a considerable increase in anomaly values, particularly in the southern and northwestern regions, exceeding 1.0 °C (Figure 7e) in 2015. In 2017, the value approached 3.0 °C in the west and reached 4.0 °C in the southeastern and southwestern regions (Figure 7f).

Overall, the basin exhibited negative PREC anomalies (Figure 8). Only negative anomalies were observed during the CHU+ season of 2011–12 (Figure 8a), particularly in the southern region, with values reaching up to 90 mm. In the subsequent period (Figure 8b), despite the southeastern region showing positive anomalies (around 90 mm), the southwestern region had negative anomalies exceeding 300 mm. In 2016–17 (Figure 8c), positive anomalies were noted in the basin, with values reaching up to 270 mm in the southwestern region. However, other areas show negative anomalies, with the highest value in the northern part of the basin. The opposite occurs regarding the ANOM in the CHU– season (Figure 8d–f). The basin mainly exhibits positive anomalies, with higher values in the southwestern region, reaching up to 60 mm (Figure 8d–f).

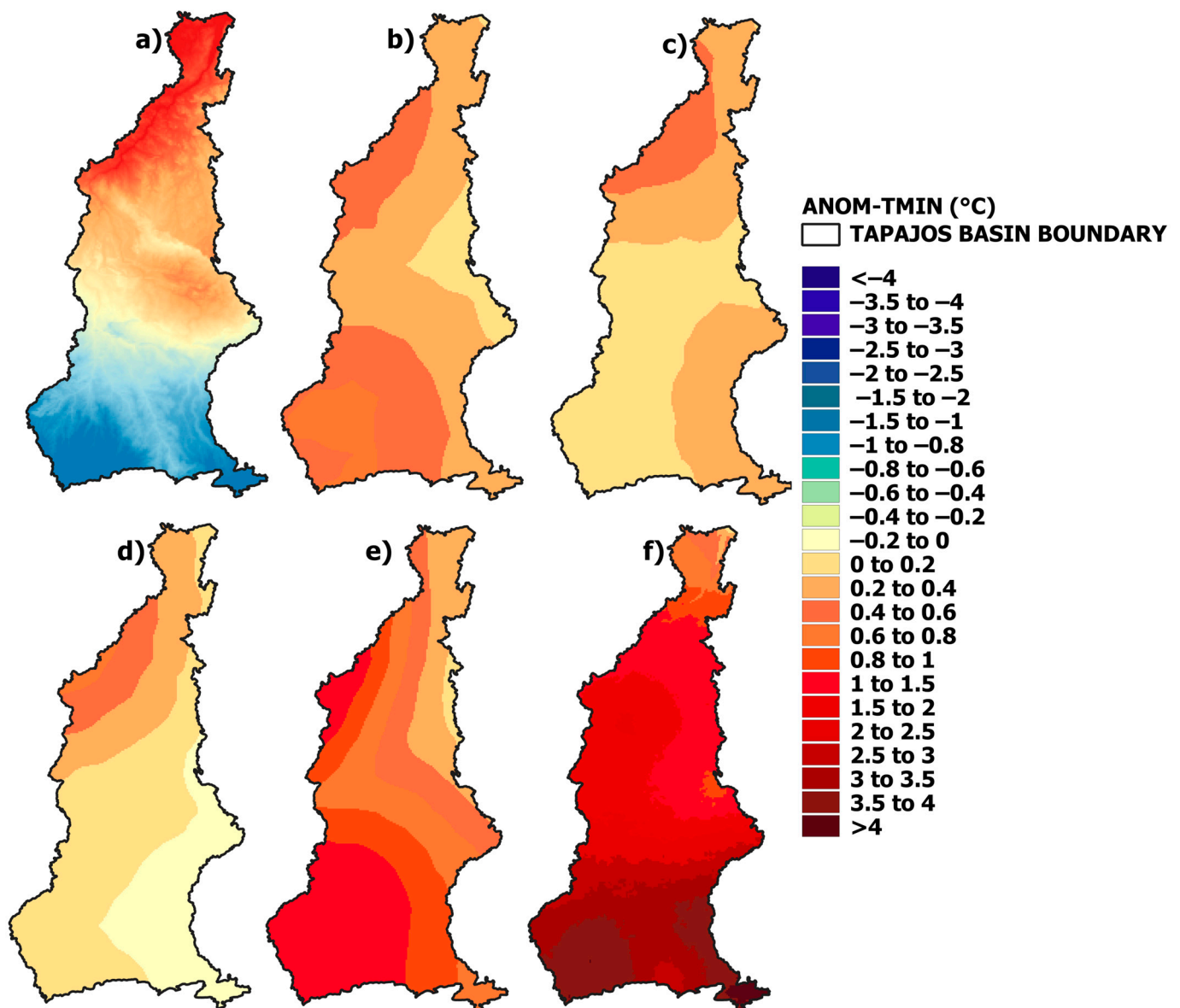


Figure 7. Minimum temperature seasonal anomaly for CHU+ (November to April) and CHU− (May to September) stations. (a–c) correspond to the CHU+ seasons of 2011–12, 2014–15 and 2016–17 and (d–f) correspond to the CHU− seasons of 2012, 2015 and 2017, respectively.

3.2. Integrated Analysis between Deforestation and Meteorological Variables

The variability of DFT data, grouped according to Kernel density, along the highways (Figure 9) indicates that the highest concentration is in the central and northeastern part of the basin in all three years, with some high-density areas in the northern portion.

In 2010, the most frequent DFT densities were low and high (Figure 9A), with high densities mainly occurring in the central and northeastern parts of the basin. In other words, medium-density areas were less prevalent. In 2013 and 2015 (Figure 9B,C), medium-density DFT areas increased, especially in the basin's northeastern and far northern parts. Additionally, there has been an overall increase in DFT density since 2010; most of this region had low-density DFT. Generally, deforestation predominantly occurs in the headwaters of the basin, concentrating from the mid-course (central portion) to the upper course, affecting areas with higher ANOM in the CHU− season (Figure 8).

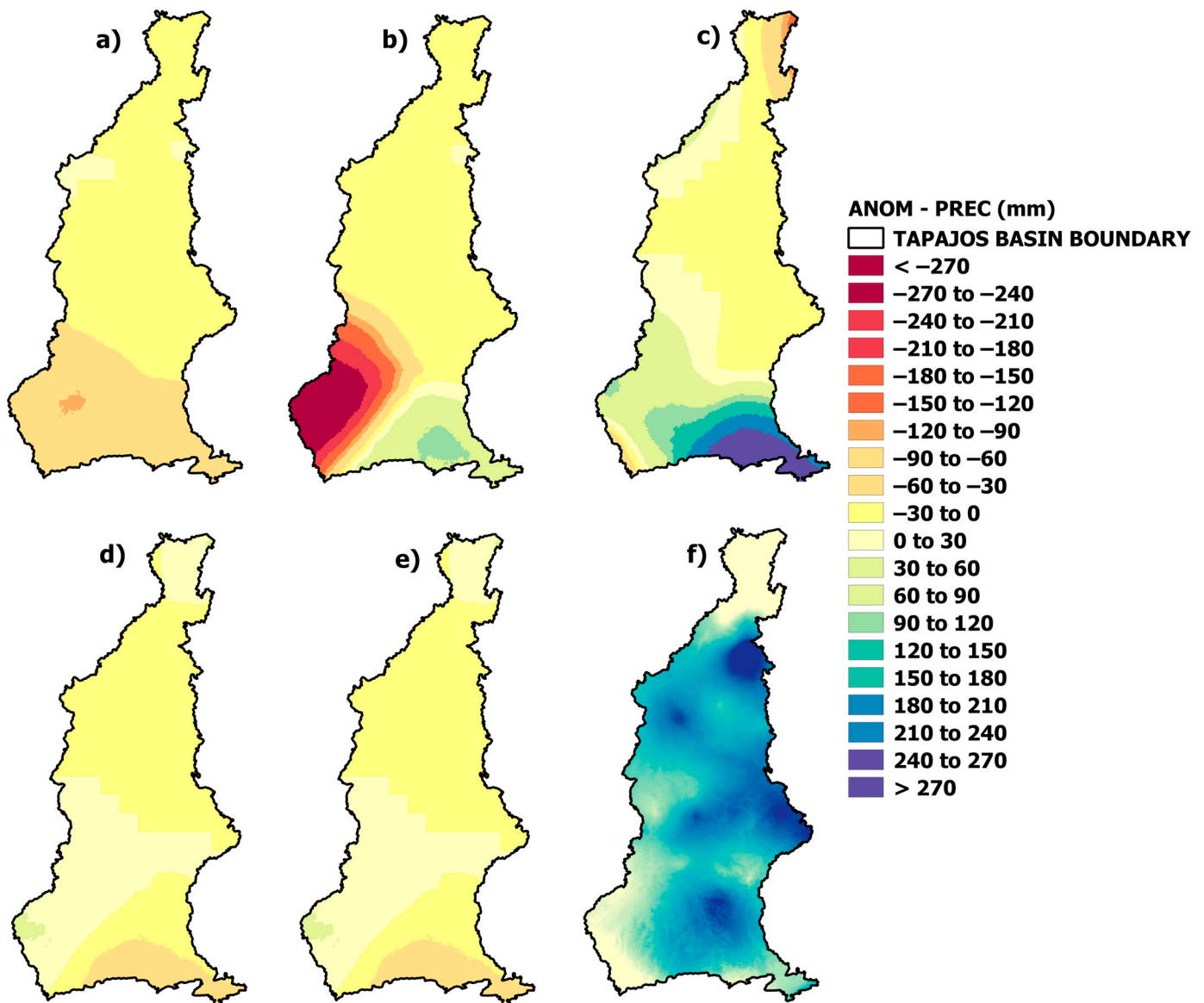


Figure 8. Precipitation seasonal anomaly for CHU+ (November to April) and CHU− (May to September) stations. (a–c) correspond to the CHU+ seasons of 2011–12, 2014–15 and 2016–17 and (d–f) correspond to the CHU− seasons of 2012, 2015 and 2017, respectively.

The correlation results (r) and coefficient of determination (R^2) between $\text{PREC} \times \text{DFT}$, $\text{TMAX} \times \text{DFT}$ and $\text{TMIN} \times \text{DFT}$ for the selected grid cells in the Lower, Middle and Upper Tapajós regions are presented in Table 2.

The most significant correlation values were found in the Middle–Lower Tapajós region for the correlations between DFT and TMAX, as well as TMIN, in both seasons (CHU+ and CHU−). Some grid cells showed mostly moderate and inverse correlations, ranging from 0.75 to -0.62 . These values indicate changes of approximately 56%, 49%, 43%, 40% and 39%, respectively, in TMAX and TMIN due to DFT. In contrast, the correlation values between $\text{DFT} \times \text{PREC}$ were less significant.

In the Upper Tapajós region, the correlation results were also the inverse; however, the values are lower when compared to the Middle–Lower Tapajós: 0.56 (31%), -0.49 (24%), -0.48 (23%) for the correlation between $\text{DFT} \times \text{TMAX}$ and TMIN, suggesting a weak correlation between $\text{DFT} \times \text{PREC}$ in this area. The more efficient response was associated with temperature and less with PREC due to the basin’s spatial variability

and distinct physiographic characteristics, particularly between the Upper–Middle and Middle–Lower regions.

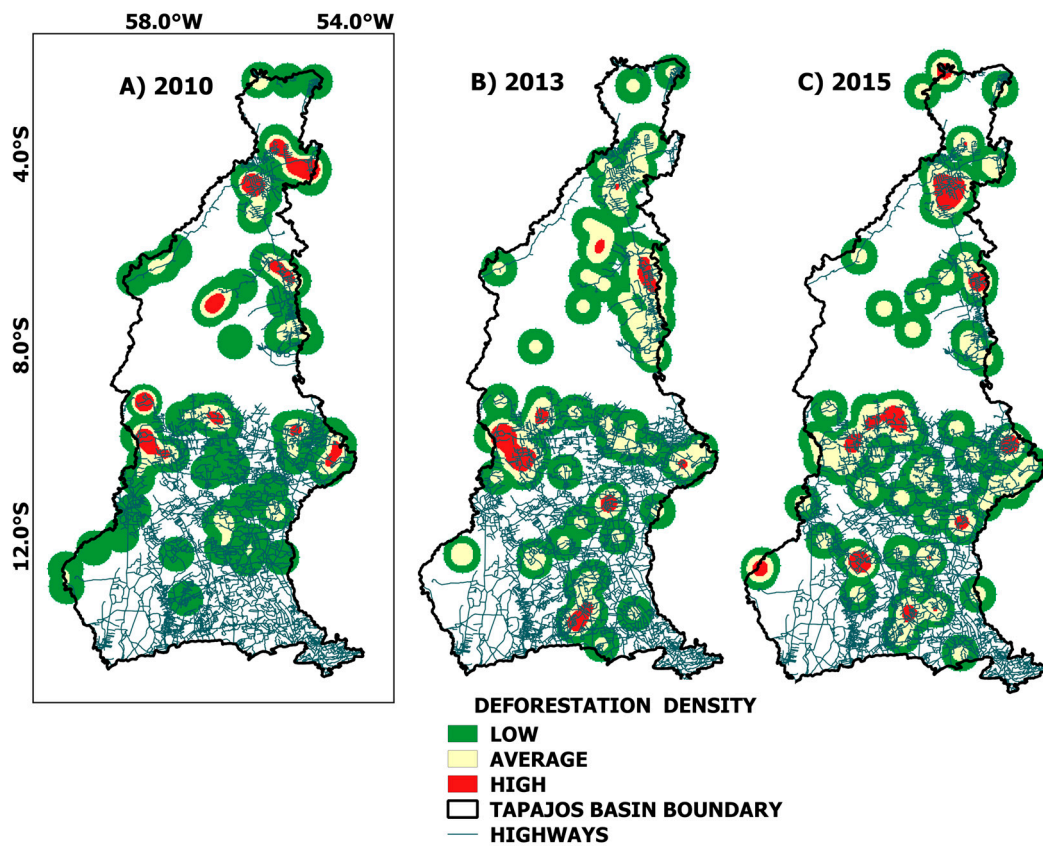


Figure 9. DFT density in the Tapajós River basin for the years 2010, 2013 and 2015.

Table 2. Results of the correlation (r) and coefficient of determination (R^2) between DTF and TMAX, DTF and DTF and PREC for the CHU+ and CHU– station, calculated in the selected grid cells of the Tapajós River sub-basins for the period from 2008 to 2018.

Sub-Basins	Squares	TMAXCHU+		TMAXCHU–		TMINCHU+		TMINCHU–		PRECCHU+		PRECCHU–	
		r	R^2	r	R^2	r	R^2	r	R^2	r	R^2	r	R^2
Low	C26	0.37	0.14	0.10	0.01	0.03	0.00	–0.21	0.04	0.13	0.02	0.39	0.15
	J24	–0.30	0.09	–0.28	0.08	–0.58	0.34	–0.51	0.26	0.34	0.11	–0.02	0.00
	L28	–0.34	0.11	–0.66	0.43	–0.43	0.19	–0.70	0.49	0.19	0.04	–0.22	0.05
	N22	–0.28	0.08	0.11	0.01	–0.04	0.00	0.37	0.14	–0.19	0.03	0.41	0.17
Average	Q22	–0.14	0.02	0.19	0.03	–0.08	0.01	0.10	0.01	–0.60	0.37	0.43	0.19
	V13	0.28	0.08	0.75	0.56	0.40	0.16	0.47	0.22	–0.19	0.04	–0.17	0.03
	Z20	0.44	0.20	0.05	0.00	0.44	0.19	0.18	0.03	–0.10	0.01	0.00	0.00
	Y26	–0.62	0.39	–0.63	0.40	–0.63	0.40	–0.61	0.37	0.00	0.00	–0.32	0.10
	AG26	–0.45	0.20	–0.14	0.02	–0.45	0.20	–0.14	0.02	–0.01	0.00	–0.24	0.06
High	AL10	–0.01	0.00	–0.20	0.04	–0.01	0.00	–0.2	0.04	–0.03	0.00	–0.11	0.01
	AM18	0.16	0.03	0.25	0.06	0.16	0.02	0.25	0.06	–0.19	0.04	–0.16	0.03
	AP10	–0.49	0.24	–0.24	0.06	–0.48	0.23	–0.24	0.06	0.08	0.01	0.01	0.00
	AS30	–0.43	0.19	–0.06	0.00	–0.43	0.19	–0.06	0.00	0.12	0.02	0.18	0.03
	BH19	0.12	0.02	0.56	0.31	0.12	0.02	0.56	0.31	–0.16	0.02	0.08	0.01

The results of the Mann–Kendall test (Table 3) show significant statistical values. In the CHU– season, the S value is negative and the p -value is below 0.05, indicating a negative

trend in PREC. In the CHU+ season, the S value is positive, indicating a positive trend in PREC.

Table 3. Results of the Mann–Kendall test for PREC, TMAX, TMIN and DFT of the CHU+ and CHU– station in the basin are shown below: PRECCHU+ (precipitation of the CHU+ station during the rainy season), PRECCHU– (precipitation of the CHU– station), TMAXCHU+ (maximum temperature of the CHU+ station during the rainy season), TMAXCHU– (maximum temperature of the CHU– station), TMINCHU+ (minimum temperature of the CHU+ station during the rainy season) e TMINCHU– (minimum temperature of the CHU– station).

Mann Kendall Test					
Variable	Statistic S	Var (S)	Tau	p-Value	Alpha
PRECCHU+	4320	2,896,013	0.099	0.01115	0.05
PRECCHU–	–4670	2,925,206	–0.106	0.00634	0.05
DFT	2600	268,666	0.333	0.1272	0.05
TMAXCHU+	4597	1,639,297	0.167	0.0003	0.05
TMAXCHU–	2615	2,590,038	0.072	0.1043	0.05
TMINCHU+	8049	2,706,214	0.211	0.0000	0.05
TMINCHU–	17,580	2,797,603	0.441	0.0000	0.05

The temperature shows a positive trend, except for TMAX in CHU–, where the *p*-values are significant (below 0.05). TMIN in CHU– stands out with a tau value of 0.44. Regarding DFT, there was no significant trend result, which could be due to the period used.

4. Discussion

The seasonal climate in the basin exhibits temperature and precipitation anomalies, with a notably high positive anomaly in TMIN (close to 4.0 °C) observed in the southern region of the basin during the CHU– season in 2017.

Although the study took place in years without the influence of the ENSO phenomenon, except for the CHU– season in 2015, the first two months coincided with the onset of the El Niño phenomenon (August and September), as CPTEC/INPE includes August of one year in the calculations up to July of the following year. Moreover, [37] considered the 2015–16 El Niño the third most intense in modern history. Considering that ENSO caused an intense dry season that significantly impacted the Amazon, it can be inferred that it likely influenced the results observed in the TMIN during the CHU– season in 2017.

In addition to the influence of natural phenomena such as El Niño, the impact of human activity in the region is noteworthy [38–43]. These authors have documented various factors that assess land use and land cover changes in the region, highlighting a rise in air temperature in the Amazon, reaching up to 3.0 °C due to deforestation. They argue that the temperature increase could reduce evapotranspiration and increase latent heat flux, among other effects.

One of the regions that experienced a considerable positive anomaly in air temperature was the northwestern part of the basin. This area is marked by significant mining activity in the state of Pará, encompassing the municipalities of Itaituba, Jacareacanga, Novo Progresso and Trairão [18,44], with a high concentration of gold extraction. Deforestation caused by mining leads to increased soil exposure, contributing to higher sensible heat flux in the region and altering the energy balance at the surface [45,46].

Regarding the results obtained in precipitation (PREC), it is worth mentioning the negative anomaly observed in various regions of the basin, especially the significant value exceeding 300 mm observed during the rainy season of 2014–15. Precipitation in the Tapajós basin, particularly in the Middle and Lower Tapajós, is directly associated with cloud bands of the Intertropical Convergence Zone (ZCIT) from March to May, while the Middle and Upper Tapajós are associated with the South Atlantic Convergence Zone (ZCAS) from October to February [47]. Therefore, for the purpose of discussion, the

following data were used: Information on the behavior of the Intertropical Convergence Zone (ZCIT) and the South Atlantic Convergence Zone (ZCAS) from the Technical Bulletins of CPTEC/INPE [48], data from the Meridional Mode of the Atlantic (MMA) [49], acquired from the NCEP/NOAA website and River flow data obtained from the Hydrological System (<http://www.snirh.gov.br/hidrotelemetria/> (accessed on 25 January 2023)) of ANA. The activity of the main precipitating phenomena present in the CHU+ season of the basin, namely the South Atlantic Convergence Zone (ZCAS) and the Intertropical Convergence Zone (ZCIT), was analyzed. Since the ZCIT is associated with the inter-hemispheric gradient (Atlantic Dipole), responsible for modulating (north–south) this phenomenon over the Atlantic Ocean, the performance of the positive (unfavorable for precipitation) and negative (favorable for precipitation) phases of the dipole was evaluated.

From the analyses of these phenomena's occurrences (episodes), it was observed that the displacement of the Intertropical Convergence Zone (ZCIT) to the northern region of the basin happened discretely when comparing the number of episodes in which the phenomenon shifted to the southern hemisphere (mostly reaching 1°S) to the episodes where it reached 3°S (extreme northern region of the basin). This was justified by the positive dipole effect (result found using the Meridional Mode of the Atlantic) during the three studied rainy periods, contributing to an unfavorable condition for the descent of the ZCIT over the Amazon and northeastern Brazil [50].

Regarding the behavior of ZCAS, it was observed in the technical reports from CPTEC/INPE [48] that there were months when the phenomenon had no episodes (for example, November 2011, October and December 2014, October, November and December 2016). In some episodes, the rainfall volumes may have been higher in the coastal and oceanic regions (located in southeastern Brazil and the South Atlantic Ocean, respectively) of the ZCAS, as the phenomenon is more active in years when ENSO occurs in its cold phase [51]. These factors may have influenced the negative PREC anomaly (327 mm) in the southwestern region of the basin in 2014–15 (a region that constitutes the Amazonian ZCAS). Furthermore, the ANOM of the flow rate in the same period (2014–15) was verified at two river gauge stations in the basin. The obtained values indicated a negative flow rate ANOM in the rainy season, both at the headwaters and at the mouth, corroborating the PREC result.

The positive PREC anomaly in the rainy season of 2014–15 in the southeastern region and in 2016–17 in the southern region of the basin may have been influenced by the action of other phenomena that affect the rainy period, such as the Upper-Level Cyclonic Vortex (VCAN), the Bolivian High (AB), the Moisture Convergence Zone (ZCOU) and Mesoscale Convective Systems (CCM) [49].

Anthropogenic activities might have also contributed to the negative findings, as deforestation has a direct relationship with increased temperature and decreased precipitation, leading to reduced evapotranspiration [52]. Ref. [53] demonstrated in their studies that deforestation in the tropics reduces precipitation in the Amazon and increases temperature. [54] concluded that precipitation in the Xingu River basin decreased by 245 mm in the last 40 years, reducing rainy days associated with high deforestation rates in the southeastern Amazon.

The results of negative ANOM of PREC, in the northwest of the basin align with the region where conservation units are located (Amazon National Park, Itaituba I and II National Forests, Crepuri National Forest and Tapajós Environmental Protection Area) that have been shrinking due to degradation from mining and hydroelectric construction in the Tapajós basin [18,55].

As for the density of DFT in the basin region for the years 2010, 2013 and 2015, it was observed that in 2010, the values were low, experiencing an increase in the last two years, primarily concentrated along the highways.

In the Tapajós basin region, there is the BR-163 highway, which was built to provide access to the interior of the Amazon, enabling the flow of people and goods. Today, its significance lies in transporting soybean production from the north-central region of

Mato Grosso to the port of Santarém, passing through preserved and indigenous areas, causing severe environmental issues [27,28]. Additionally, the basin faces other problems such as, the construction of hydroelectric dams, mining activities, logging and extensive cattle ranching.

Without asphalt, the highway has already caused significant environmental damage. With paving, the impact on the surrounding area greatly increases, accelerating the destruction of the forest not only near the highway but also in the areas under its influence [56]. The discourse of the state, aiming to bring development and sustainability through the construction of this highway, is debated in the study by [19] for the municipalities of Santarém, Itaituba, Novo Progresso (Pará states) and Sinop (Mato Grosso). In their study, the authors illustrate the hardships caused by this construction.

The correlation results showed more significant values in the Lower and Middle Tapajós, especially between DFT and temperature, which are directly related. It is worth noting that the geographical expansion of the agribusiness frontier is focused on Northern Mato Grosso, being a valid option for grain transportation, with ports like Itacoatiara (AM), Santarém (PA) and Vila do Conde-PA [57].

The comparative evaluation between Upper, Middle and Lower Tapajós, showed more negative correlations than positive ones, especially between DFT and PREC. In the Amazon region, several studies have obtained similar results. For instance, Ref. [58] found a negative correlation between DFT and PREC in the municipality of Colíder, in the state of Mato Grosso (South of the Amazon—the municipality is located within the Tapajós basin), indicating that the higher the deforested area, the lower the observed rainfall rate. Ref. [59] concluded that there is a negative linear relationship between PREC and the extent of DFT in the Amazon. Refs. [20,30] correlated PREC and DFT variables in the southern Amazon region and found significant results.

In the correlation results between DFT and PREC, it is observed that there were more significant results in the less rainy period. During this period, meteorological phenomena have no influence, unlike the rainy season, when these phenomena can interfere with the relationships between variables. Therefore, preserving the Amazon rainforest, as well as all forests, is of utmost importance for the proper and balanced functioning of ecosystems and the maintenance of biological diversity. Additionally, the forest serves significant functions such as erosion control, desertification prevention, water quality maintenance and atmospheric carbon sequestration.

Understanding the transformations that anthropogenic actions can cause in surface-atmosphere physical interactions allows for the development and creation of preservation actions, management and public policies to reduce impacts and maintain the natural services of the Tapajós River basin. Preservation studies of watersheds are essential in the global context of preservation and reducing risks and vulnerabilities associated with climate change, as replicating this analysis for other basins enables the creation of a climate-environmental scenario with greater accuracy for the Amazon region, a key biome on the agenda of major panels focused on mitigating global climate change.

5. Conclusions

In closing, the results of this study highlight the relationship between deforestation and seasonal climate in the Tapajós River Basin. Deforestation mainly occurs along the highways constructed in the region and the increase in average deforestation density can make the climate more vulnerable. These consequences are due to the crucial role of the forest in regulating the hydrological cycle and the environment.

In the research on precipitation and temperature anomalies, the results showed a negative anomaly in precipitation, being more significant in the rainy season and the opposite in the less rainy season with more discreet values. In temperature, the positive anomaly presented more significant values, especially in the basin's southern, southwestern and northwestern regions.

The results of the correlation between deforestation (DFT) and meteorological variables showed more significant values towards the north of the basin, confirming historical concerns. In other words, the accelerated deforestation in the Upper Tapajós has been spreading in recent decades to other sub-basins, especially those regions with environmental preservation areas. The basin exhibited a negative trend in precipitation (PREC) in the CHU— season and positive trends in maximum temperature (TMAX) and minimum temperature (TMIN).

It is recommended that further investigations be conducted with more regional sampling points. The basin has its particularities, such as a drainage area more extensive than 490,000 km², topographic variations, diverse climatic variables following the north–south axis of the basin, environmental fragmentation (with various altered areas alternating with forest cover) and a dense hydrographic network covering the region. Therefore, specific studies are suggested, as deforestation can negatively impact the local climate, as well as areas that rely on the atmospheric pumping performed by the forest.

Author Contributions: Conceptualization, V.d.S.F., A.M.M.d.L., R.R.S.d.O., E.B.d.S., G.R.C.S., D.C.S. and M.A.; data curation, V.d.S.F., A.M.M.d.L., R.R.S.d.O., E.B.d.S., G.R.C.S., D.C.S., M.A. and E.A.d.O.S.; formal analysis, V.d.S.F., A.M.M.d.L., R.R.S.d.O., E.B.d.S., G.R.C.S., M.A. and E.A.d.O.S.; resources, V.d.S.F., A.M.M.d.L., R.R.S.d.O., E.B.d.S., M.A. and T.S.d.S.D.; methodology, V.d.S.F., A.M.M.d.L., R.R.S.d.O., E.B.d.S., G.R.C.S., D.C.S. and M.A.; Supervision, V.d.S.F., A.M.M.d.L., R.R.S.d.O. and E.B.d.S.; validation, V.d.S.F., A.M.M.d.L., R.R.S.d.O., E.B.d.S., G.R.C.S., D.C.S., E.A.d.O.S. and T.S.d.S.D.; Writing—original draft, V.d.S.F., A.M.M.d.L. and E.B.d.S.; Writing—review and editing, V.d.S.F., A.M.M.d.L., R.R.S.d.O., E.B.d.S., G.R.C.S., D.C.S., M.A., E.A.d.O.S. and T.S.d.S.D. All authors have read and agreed to the published version of the manuscript.

Funding: This research received no external funding.

Institutional Review Board Statement: Not applicable.

Informed Consent Statement: Informed consent was obtained from all subjects involved in the study.

Data Availability Statement: <http://www.snirh.gov.br/hidrotelemetria>; <http://terrabrasilis.dpi.inpe.br>; <https://www.worldclim.org/data/worldclim21.html>; https://tempo.cptec.inpe.br/bole_timtecnico/pt; <https://psl.noaa.gov/data/timeseries/monthly/AMM/ammsst.data> (accessed on 5 September 2022).

Acknowledgments: The authors would like to thank the Pro-Rector of Research and Postgraduate Studies of the Federal University of Pará.

Conflicts of Interest: The authors declare no conflict of interest. The funders had no role in the design of the study; in the collection, analyses, or interpretation of data; in the writing of the manuscript; or in the decision to publish the results.

References

1. Wajim, J. Impacts of deforestation on socio-economic development and environment in Nigeria. *Int. J. Soc. Sci. Humanit. Invent.* **2020**, *7*, 5852–5863. [[CrossRef](#)]
2. Bologna, M.; Aquino, G. Deforestation and world population sustainability: A quantitative analysis. *Sci. Rep.* **2020**, *10*, 7631. [[CrossRef](#)] [[PubMed](#)]
3. Lawrence, D.; Vandecar, K.; Radel, C.; Schmook, B.; Schneider, L.; Rogan, J.; Geoghegan, J. When the Forest is Cut Down, Does it Matter How It is Cut? Biophysical and Socioeconomic Feedbacks of Selective Logging. *Front. For. Glob. Chang.* **2022**, *5*, e756115. [[CrossRef](#)]
4. Fazel-Rastgar, F. The Evidence of Recent Canadian Arctic Climate Change. A Case Study, the Baffin Island. *Int. J. Glob. Warm.* **2020**, *20*, 165–185. [[CrossRef](#)]
5. Alves de Oliveira, B.F.; Bottino, M.J.; Nobre, P.; Nobre, C.A. Deforestation and climate change are projected to increase heat stress risk in the Brazilian Amazon. *Commun. Earth Environ.* **2021**, *2*, 207. [[CrossRef](#)]
6. Gulizia, C.N.; Raggio, G.A.; Camilloni, I.A.; Saurral, R.I. Changes in mean and extreme climate in southern South America under global warming of 1.5 °C, 2 °C, and 3 °C. *Theor. Appl. Climatol.* **2022**, *150*, 787–803. [[CrossRef](#)]
7. Arias, P.A.; Rivera, J.A.; Sörensson, A.A.; Zachariah, M.; Barnes, C.; Philip, S. Interplay between climate change and climate variability: The 2022 drought in Central South America. *Clim. Chang.* **2023**, *177*, 6. [[CrossRef](#)]

8. Lapola, D.M.; Pinho, P.; Barlow, J.; Aragão, L.E.O.C.; Berenguer, E.; Carmenta, R.; Liddy, H.M.; Seixas, H.; Silva, C.V.J.; Walker, W.S. The drivers and impacts of Amazon forest degradation. *Science* **2023**, *379*, eabp8622. [[CrossRef](#)]
9. Matricardi, E.A.T.; Skole, D.L.; Costa, O.B.; Pedlowski, M.A.; Samek, J.H.; Miguel, E.P. Long-term forest degradation surpasses deforestation in the Brazilian Amazon. *Science* **2020**, *369*, 1378–1382. [[CrossRef](#)]
10. Bagheri, O.; Chaudhari, S.N.; Pokhrel, Y. H030-0019 Hydrological Thresholds for Sustainable Land Use and Land Cover Change in Amazon River Basin. In Proceedings of the AGU Fall Meeting Abstracts, Online, 1–17 December 2020; Volume 2020.
11. Silva, R.F.B.; Rodrigues, L.N.; Sena, A.; Santos, M.A.; Torres, G.G.; Santos, M.A.S. A Modeling Approach for Analyzing the Hydrological Impacts of the Agribusiness Land-Use Scenarios in an Amazon Basin. *Land* **2023**, *12*, 1422. [[CrossRef](#)]
12. Capitani, C.; Angelini, R.; Keppele, F.W.; Hallwass, G.; Silvano, R.A.M. Food web modeling indicates the potential impacts of increasing deforestation and fishing pressure in the Tapajós River, Brazilian Amazon. *Aquat. Ecol.* **2021**, *55*, 33. [[CrossRef](#)]
13. Barreto, J.B.; Freitas, P.B.; Fontgalland, I.L.; Macri, L.M.S.R.; Estrela, T.F. Payments for Environmental Services (PES): A study on Brazilian legislation and the structuring of agreements. *Res. Soc. Dev.* **2020**, *9*, e38791211306. [[CrossRef](#)]
14. Gillespie, T.W. Policy, drought and fires combine to affect biodiversity in the Amazon basin. *Nature* **2021**, *597*, 481–483. [[CrossRef](#)] [[PubMed](#)]
15. Ruiz-Vásquez, M.; Arias, P.A.; Martínez, J.A.; Espinoza, J.C. Effects of Amazon basin deforestation on regional atmospheric circulation and water vapor transport towards tropical South America. *Clim. Dyn.* **2020**, *54*, 4169–4189. [[CrossRef](#)]
16. Andrade, R. One River and 40+ Dams: The China Factor in the Amazonian Tapajós Waterway. In *The Political Economy of Hydropower in Southwest China and Beyond*; Palgrave Macmillan: Cham, Switzerland, 2021; pp. 275–293.
17. Théry, H. A expansão da produção de grãos e a infraestrutura de circulação no Brasil. *Rev. Política E Planej. Reg.* **2019**, *2019*, 284–305.
18. Bieri, M.L.; Picanço, V.M.P.A. Considerations of mining in Tapajós basin and impacts on Munduruku land. *Int. J. Dev. Res.* **2019**, *9*, 28622–28631.
19. Brito, R.; Castro, E. Desenvolvimento e conflitos na Amazônia: Um olhar sobre a colonialidade dos processos em curso na BR-163. *Rev. Nera* **2018**, *42*, 51–73. [[CrossRef](#)]
20. Leite-Filho, A.T.; Soares-Filho, B.S.; Davis, J.L.; Abrahão, G.M.; Börner, J. Deforestation reduces rainfall and agricultural revenues in the Brazilian Amazon. *Nat. Commun.* **2021**, *12*, e259. [[CrossRef](#)] [[PubMed](#)]
21. Le Tourneau, F.M. Is Brazil now in control of deforestation in the Amazon? *Cybergeo Eur. J. Geogr.* 2016. [[CrossRef](#)]
22. Dos Reis, M.; De Alencastro Graça, P.M.L.; Yanai, A.M.; Ramos, C.J.P.; Fearnside, P.M. Forest fires and deforestation in the central Amazon: Effects of landscape and climate on spatial and temporal dynamics. *J. Environ. Manag.* **2021**, *288*, e112310. [[CrossRef](#)]
23. Silveira, M.V.F.; Petri, C.A.; Broggio, I.S.; Chagas, G.O.; Macul, M.S.; Leite, C.C.S.; Ferrari, E.M.M.; Amim, C.G.V.; Freitas, A.L.R.; Motta, A.Z.V.; et al. Drivers of Fire Anomalies in the Brazilian Amazon: Lessons Learned from the 2019 Fire Crisis. *Land* **2020**, *9*, 516. [[CrossRef](#)]
24. Bowman, D.M.; Kolden, C.A.; Abatzoglou, J.T.; Johnston, F.H.; Van der Werf, G.R.; Flannigan, M. Vegetation fires in the Anthropocene. *Nat. Rev. Earth Environ.* **2020**, *1*, 500–515. [[CrossRef](#)]
25. Latrubesse, E.M. Quaternary megafans, large rivers and other avulsive fluvial systems: A potential “who is who” in the geological record. *Earth Sci. Rev.* **2015**, *146*, 1–30. [[CrossRef](#)]
26. Fearnside, P.M. Desmatamento na Amazônia: Dinâmica, impactos e controle. *Acta Amaz.* **2006**, *36*, 395–400. [[CrossRef](#)]
27. Neto, T.O.; Nogueira, R.J.B. A geopolítica rodoviária na Amazônia: BR-163/Santarém-Cuiabá. *Rev. De Geopolít.* **2016**, *6*, 1–21.
28. Neto, T.O. As rodovias na Amazônia: Uma discussão geopolítica. *Rev. Fr.-Bras. De Geogr.* **2019**, *501*. [[CrossRef](#)]
29. Coelho, A.; Aguiar, A.; Toledo, P.; Araújo, R.; Do Canto, O.; Folhes, R.; Adami, M. Rural landscapes and agrarian spaces under soybean expansion dynamics: A case study of the Santarém region, Brazilian Amazonia. *Reg. Environ. Chang.* **2021**, *21*, 100. [[CrossRef](#)]
30. Debortoli, N.S.; Dubreuil, V.; Hirota, M.; Rodrigues Filho, S.; Lindoso, D.P.; Nabucet, J. Detecting deforestation impacts in Southern Amazonia rainfall using rain gauges. *Int. J. Climatol.* **2017**, *37*, 2889–2900. [[CrossRef](#)]
31. Santos, V.C.; Blanco, C.; Oliveira Júnior, J.F. Distribution of rainfall probability in the Tapajós River Basin, Amazonia, Brazil. *Rev. Ambiente Água* **2019**, *14*, 3. [[CrossRef](#)]
32. Alarcon, D.F.; Millikan, B.; Torres, M. *Ocekadí: Hidrelétricas, Conflitos Socioambientais e Resistência na Bacia do Tapajós*, 2nd ed.; International Rivers Brasil: Brasília, DF, Brasil, 2016; 531p.
33. Nery, J.T.; Stivari, S.M.S.; Martins, M.L.O.F.; Silva, E.S.; Sousa, P. Estudo da precipitação do estado do Paraná e sua associação à temperatura da superfície do Oceano Pacífico. *Rev. Bras. De Agrometeorol.* **2005**, *13*, 161–171.
34. Yu, W.; Ai, T. The visualization and analysis of urban facility pois using network kernel density estimation constrained by multi-factors. *Bol. De Ciênc. Geod.* **2014**, *20*, 902–926. [[CrossRef](#)]
35. Leite Filho, A.T.; De Sousa Pontes, V.Y.; Costa, M.H. Effects of deforestation on the onset of the rainy season and the duration of dry spells in southern Amazonia. *J. Geophys. Res. Atmos.* **2019**, *124*, 5268–5281. [[CrossRef](#)]
36. Cabral Júnior, J.B.; Lucena, R.L. Análises das precipitações pelos testes não paramétricos de Mann-Kendall e Kruskal-Wallis. *Mercator* **2020**, *9*, 1–14. [[CrossRef](#)]
37. Cunha, A.P.; Marengo, J.A.; Alvala, R.C.; Deusdara-Leal, K.R.; Cuartas, L.A.; Seluchi, M.; Zeri, M.; Ribeiro-Neto, G.; Brodel, E.; Cunningham, C.; et al. *Secas e Seus Impactos No Brasil 2018*, 1st ed.; São Jose dos Campos, SP, Brasil, 2019; 19p. Available online: http://www2.cemaden.gov.br/wp-content/uploads/2019/01/Boletim_Anual_SECAS_f.pdf (accessed on 5 September 2022).

38. Nobre, C.A.; Sellers, P.J.; Shukl, A.J. Amazonian deforestation and regional climate change. *J. Clim.* **1991**, *4*, 957–988. [[CrossRef](#)]
39. Werth, D.E.; Avissar, R. The local and global effects of Amazon deforestation. *J. Geophys. Res.* **2002**, *107*, D20. [[CrossRef](#)]
40. Voldoire, A.; Royer, E.J.F. Tropical deforestation and climate variability. *Clim. Dyn.* **2004**, *22*, 857–874. [[CrossRef](#)]
41. Sampaio, G.; Nobre, C.; Costa, M.H.; Satyamurty, P.; Soares-Filho, B.S.; Cardoso, M. Regional climate change over eastern Amazonia caused by pasture and soybean cropland expansion. *Geophys. Res. Lett.* **2007**, *34*, L17709. [[CrossRef](#)]
42. Gloor, M.; Barichivich, J.; Ziv, G.; Brienen, R.; Schöngart, J.; Peylin, P.; Barcante Ladvoat Cintra, B.; Feld Pausch, T.; Phillips, O.; Baker, J. Recent Amazon climate as background for possible ongoing and future changes of Amazon humid forests. *Glob. Biogeochem. Cycles* **2015**, *29*, 1384–1399. [[CrossRef](#)]
43. Baker, J.; Spracklen, D. Climate benefits of intact Amazon forests and the biophysical consequences of disturbance. *Front. For. Glob. Chang.* **2019**, *2*, 1–13. [[CrossRef](#)]
44. Souza-Filho, P.W.M.; de Lucia Lobo, F.; Barbosa Lopes Cavalcante, R.; Mota, J.A.; da Rocha Nascimento, W., Jr.; Santos, D.C.; Siqueira, J.O. Land-use intensity of official mineral extraction in the Amazon region: Linking economic and spatial data. *Land Degrad. Dev.* **2021**, *32*, 1706–1717. [[CrossRef](#)]
45. Silvério, D.V.; Brando, P.M.; Macedo, M.N.; Beck, P.S.; Bustamante, M.; Coe, M.T. Agricultural expansion dominates climate changes in southeastern Amazonia: The overlooked non-GHG forcing. *Environ. Res. Lett.* **2015**, *10*, 104015. [[CrossRef](#)]
46. Macdougall, A.H.; Beltrami, H. Impact of deforestation on subsurface temperature profiles: Implications for the borehole paleoclimate record. *Environmental. Res. Lett.* **2017**, *12*, 074014. [[CrossRef](#)]
47. Santos, C.; Araújo, I.B.; Wanzeler, R.T.S.; Serrão, E.A.O.; Farias, M.H.C.S.; Lima, A.M.M. Regionalização hidroclimatológica da bacia hidrográfica do Rio Tapajós. *Rev. Geogr. Acad.* **2015**, *9*, 32–51. [[CrossRef](#)]
48. CPTEC/INPE. Centro de Previsão de Tempo e Estudos Climáticos. Instituto Nacional de Pesquisas Espaciais. Available online: <https://tempo.cptec.inpe.br/boletimtecnico/pt> (accessed on 2 November 2021).
49. Cavalcanti, I.F.A. *Tempo e clima no Brasil*, 2nd ed.; Oficina de Textos: São Paulo, SP, Brasil, 2016; 464p.
50. Silva, F.F.; Dos Santos, F.A.; Dos Santos, J.M. Índice de anomalia de chuva (IAC) aplicado ao estudo das precipitações no município de caridade, Ceará, Brasil. *Rev. Bras. De Climatol.* **2020**, *27*, 426–442. [[CrossRef](#)]
51. Carvalho, L.M.V.; Jones, C.; Liebmann, B. The South Atlantic convergence zone: Intensity, form, persistence, and relationships with intraseasonal to interannual activity and extreme rainfall. *J. Clim.* **2004**, *17*, 88–108. [[CrossRef](#)]
52. Spera, S.A.; Galford, G.L.; Coe, M.T.; Macedo, M.N.; Mustard, J.F. Land-use change affects water recycling in Brazil’s last agricultural frontier. *Glob. Chang. Biol.* **2016**, *22*, 3405–3413. [[CrossRef](#)]
53. Bathiany, S.; Claussen, M.; Brovkin, V.; Raddatz, T.; Gayler, V. Combined biogeophysical and biogeochemical effects of large-scale forest cover changes in the MPI Earth system model. *Biogeosciences* **2010**, *7*, 1383–1399. [[CrossRef](#)]
54. Rizzo, R.; Garcia, A.S.; Vilela, V.M.D.F.; Ballester, M.V.R.; Neill, C.; Victoria, D.C.; Coe, M.T. Land use changes in Southeastern Amazon and trends in rainfall and water yield of the Xingu River during 1976–2015. *Clim. Chang.* **2020**, *162*, 1419–1436. [[CrossRef](#)]
55. Verdum, R.; Gamboa, C.; Bebbington, A.J. *Assessment and Scoping of Extractive Industries and Infrastructure in Relation to Deforestation: Amazonia*, 1st ed.; Derecho, Ambiente y Recursos Naturales (DAR): Lima, Peru, 2019; 81p.
56. Fearnside, P.M. Brazil’s Cuiabá-Santarém (BR-163) Highway: The environmental cost of paving a soybean corridor through the Amazon. *Environ. Manag.* **2007**, *39*, 601–614. [[CrossRef](#)]
57. Souza, M.M.; Rocha, M.P.; Farias, V.; Tavares, H. Optimization of soybean outflow routes from Mato Grosso, Brazil. *Int. J. Innov. Educ. Res.* **2020**, *8*, 2. [[CrossRef](#)]
58. Bonini, I.; Rodrigues, C.; Dallacort, R.; Marimon Junior, B.H.; Carvalho, M.A.C. Rainfall and deforestation in the municipality of Colíder, southern Amazon. *Rev. Bras. De Meteorol.* **2014**, *29*, 483–493. [[CrossRef](#)]
59. Spracklen, D.V.; Garcia-Carreras, L. The impact of Amazonian deforestation on Amazon basin rainfall. *Geophys. Res. Lett.* **2015**, *42*, 9546–9552. [[CrossRef](#)]

Disclaimer/Publisher’s Note: The statements, opinions and data contained in all publications are solely those of the individual author(s) and contributor(s) and not of MDPI and/or the editor(s). MDPI and/or the editor(s) disclaim responsibility for any injury to people or property resulting from any ideas, methods, instructions or products referred to in the content.